JOURNAL OF APPLIED ELECTROCHEMISTRY 13 (1983) 569–575

Energy consumption of aluminium smelting cells containing solid wetted cathodes

R. C. DORWARD

Kaiser Aluminum and Chemical Corporation, Pleasanton, California 94566, USA

Received 13 October 1982

Tests with 10 kA pilot cells show that substituting a wetted, dimensionally stable cathode for the turbulent metal cathode allows the anode–cathode distance (ACD) to be decreased, with an attendant voltage reduction of about 1 V, depending on current density. Since high current efficiency is retained, specific energy consumption is decreased by about 20%. These savings are not as great as anticipated, however, because the effective electrical resistivity of the electrolyte increases as the ACD is lowered. This effect is ascribed to an increased void fraction of anode gas in the interpolar space, which appears to be dependent on anode size.

1. Introduction

The Hall–Héroult smelting process, in which alumina is dissolved in molten $NaF–AlF_3$ at 940–980° C and electrolytically decomposed by passage of direct current, has endured for almost a century as the only commercial means of producing aluminium. Largely as a result of ohmic losses through solid and liquid cell components, a moderately high specific energy input is required (the US industry average is $\simeq 16.5\ kWh\ kg^{-1}$). Although the average US specific energy consumption has been reduced by about 30% over the past 20 years, significant further savings with present technology appear possible only in newly constructed smelters (modern cells are operating near $13\ kWh\ kg^{-1}$). Unfortunately, it is unlikely that the number of these cells will be great enough to have a major impact on the industry's average energy usage in the near future. Hence, there is a large incentive to upgrade existing smelters.

The specific energy consumption of a reduction cell (in $kWh\ kg^{-1}$) is given by

$$E_s = \frac{298 V_c}{CE}, \qquad (1)$$

where V_c is the total cell voltage and CE is the current efficiency expressed as a percentage. The cell voltage may be divided into various components so that

$$E_S = \frac{298}{CE}\left(V_d + V_b + \sum V_i\right), \qquad (2)$$

where V_d is the decomposition voltage (reversible component plus overvoltage), V_b the ohmic voltage drop in the interpolar space ('bath' drop) and V_i the ohmic voltage drops in the bus bars, anode, lining, etc.

In typical smelters the bath drop accounts for 60–70% of the total ohmic energy consumption. Since V_b is related to current density, I_d; anode–cathode distance, ACD; and bath electrical resistivity, ρ:

$$V_b = I_d \rho \mathrm{ACD}, \qquad (3)$$

significant changes in one or more of these parameters will have a corresponding effect on ohmic energy consumption. Heat balance considerations preclude major reductions in the current density of existing cells (this would also have the economic disadvantage of reducing productivity). Bath resistivity is controlled by electrolyte composition, which has generally been optimized for a number of operational reasons. Reducing the anode–cathode distance therefore appears to be the only possible means of significantly lowering specific energy consumption.

The ACD in conventional smelters must be maintained above about 4 cm to prevent intermittent shorting between the anode and the turbulent metal pool, which serves as the cell cathode.

0021-891X/83 $03.00 + .12.

Table 1. Summary of pilot cell results

Cell	*Cathode*	*ACD* (cm)	*Current* (kA)	*Cell voltage* (V)	*Current efficiency,* (%)	*Specific energy consumption,* DC(kWh kg^{-1})
S1	Solid	5.2	10.01	4.85	82.5	17.49
		2.8	11.94	4.42	82.0	16.06
S2	Solid	2.8	12.84	4.87	86.1	16.85
		1.9	14.45	4.70	83.4	16.78
		1.9	14.59	4.88	88.5	16.41
S3	Solid	2.8	12.33	4.87	86.7	16.74
		2.0	13.00	4.57	86.8	15.68
		1.9	13.29	4.67	86.9	16.01
S4	Solid	2.7	13.49	4.93	84.6	17.36
		2.7	13.66	4.89	85.6	17.00
		1.8	14.85	4.74	80.5	17.53
L1	Metal	5.4	10.25	4.95	86.4	17.07

However, the use of a dimensionally stable cathode, could in principle allow the ACD to be reduced to 1.5–2.0 cm, with projected energy savings of over 20%. The discovery in the early 1950s that the electrically conductive refractory 'hard metals' are wetted by molten aluminium, while being resistant to dissolution, offered the possibility of achieving this objective [1]. Of this class of materials, titanium diboride (TiB_2) and titanium carbide (TiC) offered the most promise [2].

Over the past 20 years we have conducted a number of pilot cell campaigns to test the concept of a solid wettable cathode. This paper summarizes the findings of these tests.

2. Pilot cell results

The first five pilot cells, of nominal 10 kA capacity, were of the 'Ransley-well' design, in which the metal deposits on a slightly sloped cathode surface and drains into a centre collection trench. Each cell contained four anodes of 39 x 51 cm cross section. Table 1 gives the averaged operating data for cells S1 to S4 (solid cathodes) and a liquid metal cathode cell of the same size. Operating periods for the solid cathode cells were of 2–4 weeks duration at each ACD listed; the data for the conventional cell was averaged over 36 weeks (11 test periods). The lowest voltage was achieved with S1 cell: 4.42 V at a 2.8 cm ACD and an anode current density (CD) of 1.5 A cm^{-2} (based on 'new' anode dimensions). Cell S3 showed the best energy efficiency: 15.68 kWh kg^{-1} at a 2.0 cm ACD and an anode CD of 1.63 A cm^{-2}. Both S2 and S3 cells demonstrated that high current efficiency (87–88.5%) can be achieved at an ACD of 1.9 cm. This is especially noteworthy in view of the relatively high NaF/AlF_3 cryolite ratios (1.35–1.5 by weight) and temperatures ($\simeq 970^\circ$ C) used in these tests. (Current efficiency increases with decreasing cryolite ratio and temperature.)

It is important to recognize that the voltages and specific energy ratings of pilot cells cannot be taken at face value, because their heat balance characteristics require that they be run at higher current densities than larger cells. This, in turn, results in larger ohmic voltage drops than would be experienced in a commercial cell. Furthermore, comparisons of E_s at different ACD's are difficult because as the interpolar distance is decreased, the cell current must be increased to compensate for the lower heat generation.* The increased current, of course, is manifested by higher productivity ratings as shown in Fig. 1.

To make quantitative estimates of cell performance, the data must be normalized with respect to current density and bath resistivity. First, it is helpful to isolate the bath voltage drop as defined by

$$V_b = V_c - V_d - \sum V_i, \qquad (4)$$

where the decomposition voltage is taken to be 1.75 V (a well-accepted value for alumina elec-

* This would also apply to a large commercial cell, i.e., part of the benefit of a smaller ACD can be taken as an increase in productivity (kg per cell-day).

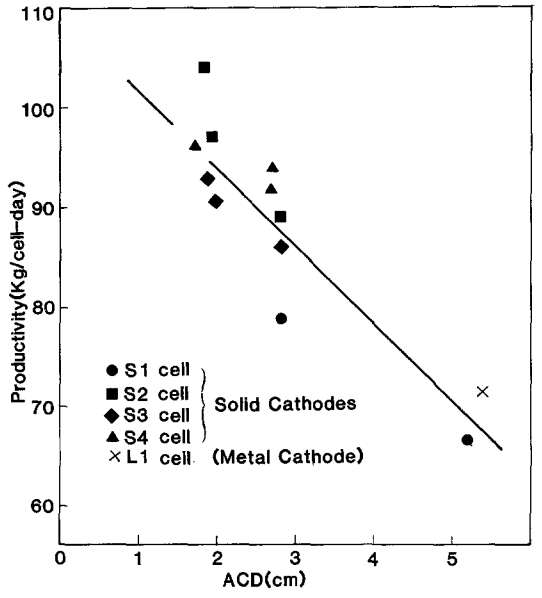

Fig. 1. Effect of anode–cathode distance on productivity of 10 kA pilot cells containing solid wettable cathodes.

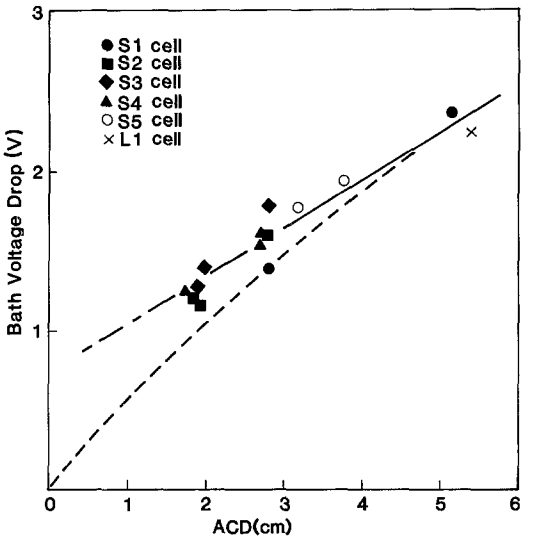

Fig. 2. Effect of ACD reduction on bath voltage drop in 10 kA pilot cells containing solid wettable cathodes. Data are normalized to an anode current density of 1.28 A cm^{-2} and a specific electrolyte resistivity of 0.408 Ω cm. Dashed line shows expected relationship corrected for current fanning effects.

trolysis) and V_i are measured and/or calculated from experimental electrical resistivity data. For comparative purposes, the bath voltage drops will be normalized to that of the conventional metal cathode Cell L1:

$$V_b(\text{norm}) = V_b\left(\frac{\rho_{L1}}{\rho} \cdot \frac{I_{L1}}{I}\right), \qquad (5)$$

where ρ is calculated from the regression equation of Choudhary [3]. The other ohmic voltage drops (ΣV_i) can be similarly treated to obtain normalized specific energy ratings for each cell.

The results of these calculations are shown graphically as a function of ACD in Figs. 2 and 3. Also included are two data points for a fifth solid cathode cell, which are based on interpolar resistance measurements. It is apparent that a voltage reduction of about 1 V can be achieved by reducing the ACD from 5 cm to 1.75 cm (at an anode CD of 1.28 A cm^{-2} and bath resistivity of 0.408 Ω cm). Estimates for other values of I_d and ρ can be obtained from Equation 5, i.e.,

$$\Delta V \simeq 1.0\left(\frac{\rho}{0.408} \frac{I_d}{1.28}\right).$$

The normalized E_s data indicate that reducing the ACD from 5 cm to 1.75 cm could lower specific energy consumption by about 20%. However, care must be taken in applying this estimate to a commercial cell because it assumes equivalent ohmic voltage drops (ΣV_i) in pilot and large cells.

Note that the bath voltage drop (Fig. 2) does not extrapolate to 0 V at 0 cm ACD. One reason for this observation is related to current 'fanning' effects, i.e., the effective cross sectional area of the interpolar space is greater than the projected area of the anode sole. The larger the ACD, the greater the effective cross-sectional area, and the smaller the anode the larger the effect. From reference electrode measurements, Haupin has estimated a fanning factor [4], which is defined as an extension in each direction to be added to the dimensions of the anodes. The dashed line in Fig. 2 shows how the bath voltage drop would be expected to change with ACD when this effect is taken into account. The majority of the data lie above this curve, suggesting the presence of another contribution to interpolar resistance at low ACD's. A convenient way of expressing this deviation from expected behaviour is to calculate the ratio V_b(actual)/V_b(expected); this is equivalent to $\bar{\rho}/\rho_5$, where $\bar{\rho}$ is the effective (actual) bath resistivity at reduced ACD and ρ_5 is the bath resistivity at 5 cm ACD. Figure 4 shows a $\bar{\rho}/\rho_5$ versus ACD plot for the V_b data in Fig. 2.

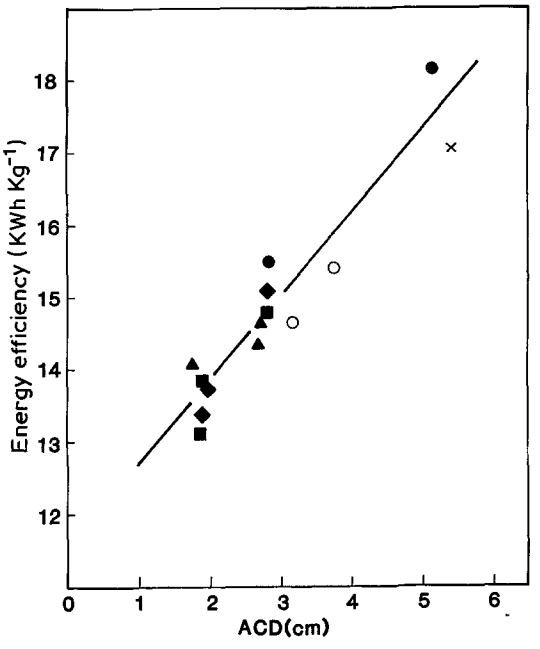

Fig. 3. Effect of ACD reduction on specific energy consumption of 10 kA pilot cells. Symbols are the same as in Fig. 2. Data are normalized to an anode current density of 1.28 A cm^{-2} and a specific electrolyte resistivity of 0.408 Ω cm.

To investigate the relationship between $\bar{\rho}/\rho_S$ and ACD further, a series of interpolar resistance measurements were conducted on another pilot cell. This cell contained cathode assemblies that corresponded on a one-to-one basis with individual anodes, rather than a monolithic cathode bottom. Cathode areas were about the same as the projected anode areas, thereby minimizing current fanning effects. The electrodes were sloped 5° (to horizontal) in an effort to promote effective gas evolution and electrolyte mixing in the interpolar space. The interpolar voltage ($V_d + V_b$) was

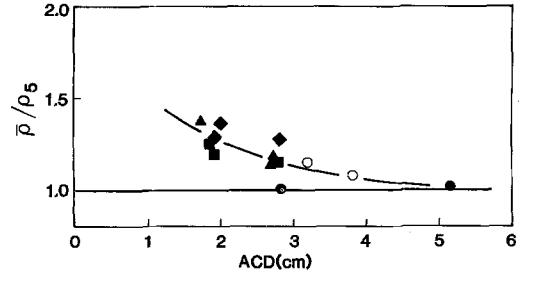

Fig. 4. Effect of ACD reduction on effective bath resistivity relative to resistivity at 5 cm ACD. Symbols are the same as in Fig. 2.

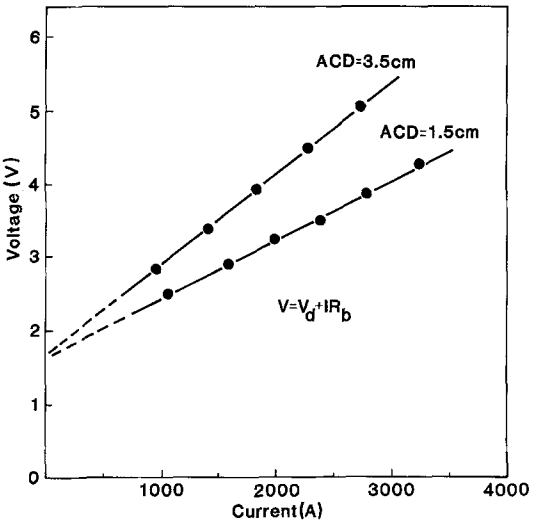

Fig. 5. *V–I* plots for close-packed bar cathode assembly. Voltage was measured between metal pool and a probe in the anode.

measured between a voltage probe in the anode about 2 cm from the sole and another probe in the metal pool below the cathode. Voltage–current (*V–I*) data were generated by reducing the electrolysis current incrementally from about 3000 A per anode (≃ 1.6 A cm^{-2}). Ignoring the small voltage drop between the probe and the bottom of the anode, the bath resistance is then determined from the slope of the *V–I* plot, i.e.,

$$V = V_d + IR_b. \tag{6}$$

Figure 5 shows *V–I* plots for ACD's of 1.5 and 3.5 cm that were measured on a close-packed 7.5 cm diameter bar assembly. The plots were linear above about 1000 A (≃ 0.5 A cm^{-2}), allowing good comparative estimates of interpolar resistance to be made. Figure 6 gives the results of three separate tests, two on the close-packed bar assembly, and the third on a flat plate assembly. Again, it is obvious that the resistance values do not extrapolate to zero at 0 cm ACD. Furthermore, the resistances are considerably greater than those depicted by the dashed line, which were calculated from the specific bath resistivity and estimated interpolar cross-sectional area (taken to be the average of the anode and cathode areas, with no fanning effects). The discrepancy between the estimated (calculated) and the apparent (measured) values increase as the ACD is decreased. Figure 7 shows how $\bar{\rho}/\rho_S$ for these data changes with ACD.

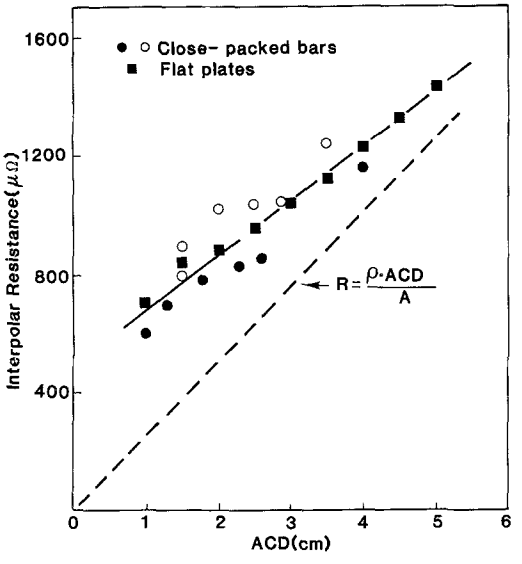

Fig. 6. Effect of ACD on interpolar resistance of 10 kA pilot cell containing 5° sloped electrode system.

The increase in effective bath resistivity with reduced ACD is more pronounced than in the previous tests (dashed line).

3. Discussion

The foregoing results show that reasonably attractive energy savings can be achieved by substituting a wettable, dimensionally stable cathode for the turbulent metal cathode. However, there is not a one-to-one correspondence between ACD reduction and decrease in interpolar resistance. For one thing, current 'fanning' effects result in a smaller effective cross-sectional area at low electrode spacings. More importantly though, there appears to be a 'polarization' effect, whereby the effective bath resistivity increases as the ACD is reduced. In one set of pilot cell tests, the effective resistivity at an ACD of 1.9 cm was about 30% higher than that at a 5 cm ACD. In another series of evaluations, the corresponding increase was about 55%. Ignoring current fanning effects, the latter situation implies that for a typical bath resistivity of 0.45 Ω cm and a current density of 1.0 A cm^{-2}, decreasing the ACD from 5 cm to 1.9 cm would give a 0.9 V saving rather than 1.4 V.

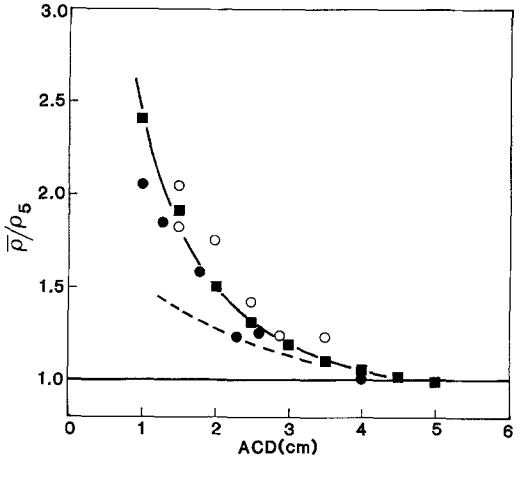

Fig. 7. Effect of ACD reduction on effective bath resistivity of 10 kA pilot cell with 5° sloped electrodes. Dashed line shows relationship for previous cells (Fig. 4).

One possible explanation for the increase in effective bath resistivity at reduced ACD is related to anode gas evolution. Considering the large rate of gas generation in a reduction cell ($\simeq 0.25$ cm^3 A^{-1} s^{-1}), the gas phase volume fraction must rise as the ACD is decreased, unless the transport velocity increases correspondingly. Russian investigators have reported specific gas volumes (ratio of gas volume in the interpolar space to the area of the anode bottom) of 0.3–0.6 cm^3 cm^{-2} under pilot cell anodes, depending on current density and depth of anode immersion [5]. The effective resistivity of the interpolar gap is obviously affected by the amount of gas in this region. The simple case of a uniformly distributed gas phase is described by the Bruggemann equation [6]:

$$\bar{\rho} = \rho(1-\epsilon)^{-3/2} \qquad (7)$$

where $\bar{\rho}$ and ρ are the resistivities of the gas-containing and gas-free electrolyte, respectively, and ϵ is the volume fraction of gas in the electrolyte. Therefore, for a constant volume of gas under an anode, the effective resistivity ($\bar{\rho}$) must increase as the ACD is decreased.* A uniform gas dispersion in the interpolar space as the above model assumes is unlikely; a more probable situation is a layer of gas-rich electrolyte near the anode surface. This case can be approximated by the following expression:

$$\bar{\rho}/\rho = 1 + \frac{\delta}{ACD}\left[\left(1-\frac{v}{\delta}\right)^{-3/2} - 1\right], \qquad (8)$$

where δ is the thickness of the gas-filled layer

* This effect is well recognized in chlorine cell technology [7].

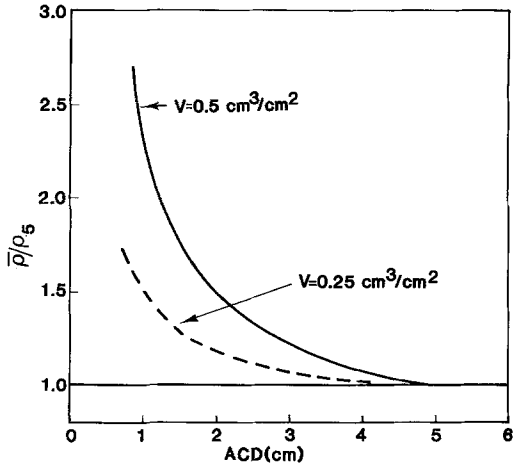

Fig. 8. Effect of gas under 1800 cm² anode on effective bath resistivity (Equation 8). It is assumed gas layer is 1 cm thick.

and v is the specific volume of the gas. Setting $\delta = 1$ cm, this equation predicts behaviour remarkably similar to that observed, compare Fig. 8 with Figs. 4 and 7.

The void fraction theory may also explain the difference between the two sets of pilot cell data. In the latter tests (Fig. 7) the anodes were sloped 5° in the width direction, so the gas flow would be largely unidirectional, thereby effectively doubling transit distance. (Normally, anodes 'wear' so that they have a slight radial slope, resulting in multi-directional gas evolution.) And since an incline of only 5° would not have a great effect on flow rate [8], the average bubble transit time would also be increased. In other words, the results are representative of an anode larger than that used in the study. Anode size and shape are known to have an effect on gas volume [9, 10]; as Fig. 8 shows, doubling the volume of anode gas would have the effect observed.

Based on the one-dimensional conduction equation, Fig. 6 indicates that a residual resistance effect exists at ACD's of 5 cm and greater. This is predicted from Equation 8, and moreover, is consistent with 'bubble resistance' voltages of 0.2 to 0.35 V that Haupin measured in a 10 kA pilot cell [4]. These values amount to 10–15% of the total ohmic interpolar voltage trop in a typical cell, and might be expected to be even greater with larger anodes.

Although the void fraction theory qualitatively describes the type of behaviour observed, the linearity of the V–I plots does not fit the model. Since the rate of gas evolution is proportional to current, the resistance of the interpolar space (slope of the V–I plot) should be dependent on current. It is possible that the expected upward curvature in the plots would be minimized by a current (or gas volume) dependent transport velocity, i.e., the higher the current, the greater the rate of bubble removal from the interpolar space. Although such behaviour has been observed in commercial smelters [11] and laboratory $PbCl_2$–KCl cells [12], we cannot rule out other current inhibiting factors such as concentration polarization, or reaction and charge transfer overvoltage, which in turn could be depdendent on bubble effects [13, 14] as has been demonstrated in chlorine cells [15]. In an attempt to minimize concentration polarization, a test was conducted with a cathode assembly containing an open array of TiB_2 parts rather than a flat monolithic structure. The results were similar to those shown in Fig. 6; if, in fact, the 'polarization' effect was reduced, it perhaps was mitigated by a restricted cathode area.

4. Summary and conclusions

Pilot Hall–Héroult cells containing dimensionally stable cathodes have demonstrated:

1. Successful operation at reduced anode–cathode distance (1.9 cm), while retaining high current efficiency.

2. Productivity increases of 20–30% at somewhat lower specific energy consumption than a conventional pilot cell with a liquid metal cathode.

At the same current density, the pilot cell results translate to a 15–25% reduction in specific energy consumption. The savings are not as great as anticipated, however, because reducing the ACD increases the effective electrical resistivity of the electrolyte. This effect, which appears to be dependent on anode size, may be due to an increased void fraction of anode gas in the interpolar space.

Acknowledgements

The efforts of D. W. Dow, W. H. Goodnow, R. A. Lewis and J. R. Payne are gratefully acknowledged for their extensive conceptual and/or experimental

contributions to this study. The US Department of Energy (Contract DE-AC03-76CS40215) partially funded a portion of the programme.

References

[1] C. E. Ransley, US Patent 3,028,324 (1962).
[2] *Idem*, in 'Extractive Metallurgy of Aluminum', Vol. 2, (edited by G. Gerard), Interscience publishers, New York (1963) p. 487.
[3] G. Choudhary, *J. Electrochem. Soc.* **120** (1973) 381.
[4] W. E. Haupin, *J. Metals* **23** (1971) 46.
[5] W. S. Siraev, D. V. Forsblom and D. Ya. Khalpakchi, *Tsvet. Met.* **49** (1976) 33.
[6] R. E. DeLaRue and C. W. Tobias, *J. Electrochem. Soc.* **106** (1959) 827.
[7] R. B. MacMullin, in 'Chlorine, Its Manufacture, Properties and Uses', (edited by J. S. Sconce), Reinhold Publishing Corp. New York (1962) p. 127.
[8] G. Kreysa and H. J. Külps, *J. Electrochem Soc.* **128**, (1981) 979.
[9] M. K. Kulesh, A. A. Dmitriev and V. O. Volodchenko, *Tsvet. Met.* **43** (1970) 23.
[10] V. V. Nerubashchenko, L. N. Antipin and A. V. Kuleshova, *ibid.* **40** (1967) 53.
[11] A. I. Begunov, *Izv Vus Tsvet. Met.* **19** (1976) 29.
[12] V. A. Kryukovskii, P. V. Polyakov, G. V. Forsblom, A. M. Tsyplakov and V. V. Burnakin, *Tsvet. Met.* **45** (1972) 62.
[13] E. W. Dewing and E. Th. van der Kouwe, *J. Electrochem. Soc.* **122** (1975) 358.
[14] P. J. Sides and C. W. Tobias, *ibid.* **127** (1980) 288.
[15] S. Okada, S. Yoshizawa, F. Hine and Z. Takehara, *J. Electrochem. Soc. Japan* **26** (1958) 165.